

***Antidesma bunius* aqueous crude extract promotes cell death via modulation of redox-sensitive and autophagy-associated genes in HCT 116 human-derived colorectal cancer cells**

Sol Joaquin Benigno¹, Glenn Oyong², Josafat John Licayan¹ and Rodolfo Sumayao Jr.^{1,*}

¹Chemistry Department, De La Salle University, 2401 Taft Avenue, Manila 0922, Philippines

²Center for Natural Sciences and Ecological Research (CENSER), De La Salle University, 2401 Taft Avenue, Manila 0922, Philippines

*Corresponding author: rodolfo.sumayao@dlsu.edu.ph

Received: July 3, 2020; Revised: August 24, 2020; Accepted: August 25, 2020; Published online: August 27, 2020

Abstract: *Antidesma bunius* fruit was previously shown to exhibit antioxidant properties, but its anticancer activities remain underexplored. We hypothesized that the phytochemicals in this fruit can influence mitochondrial integrity and can modulate stress-responsive genes in cancer cells. The present study investigated the effects of *A. bunius* fruit aqueous crude extract (*A. bunius* ACE) on the viability, redox status, and mitochondrial transmembrane potential (MTP) using a colorectal cancer cell line, HCT 116. The expression of key genes associated with oxidative stress and autophagy was also determined. Treatment of cells with *A. bunius* ACE resulted in a ~27% reduction in viability, coupled with a marked decrease in oxidative stress index by ~59%. This was accompanied by the upregulation of *NRF2* and *NRF2*-dependent genes. MTP increased ~3-fold in response to *A. bunius* ACE. The expression of *BECLIN1*, *ATG5*, and *LC3* genes also increased. Our results indicate that the phytochemicals in *A. bunius* fruits enhance mitochondrial integrity and modulate the expression of stress-responsive genes, which may be responsible for the mitigation of oxidative stress in cancer cells. These alterations may be involved in the cascade of events leading to cancer cell death effected by *A. bunius*.

Keywords: *Antidesma bunius*; colorectal cancer; oxidative stress; antioxidants; autophagy; mitochondria

Abbreviations: colorectal cancer (CRC); aqueous crude extract (ACE); mitochondrial transmembrane potential (MTP); reactive oxygen species (ROS); nuclear factor erythroid 2-related factor 2 gene (*NRF2*); glutathione peroxidase 1 gene (*GPX1*); thioredoxin reductase 1 gene (*TRXR1*); coiled-coil myosin-like BCL2-interacting protein gene (*BECLIN1*); autophagy related 5 gene (*ATG5*); microtubule-associated protein 1A/1B-light chain 3 gene (*LC3*); total phenolic content (TPC); total flavonoid content (TFC)

INTRODUCTION

Antidesma bunius is a wild berry that belongs to the *Euphorbiaceae* family and is commonly found in dip-terocarp forested areas throughout southeast Asia. Its small ovoid-shaped fruits are bright red-to-purple in color when ripe, with a distinctive mixture of sweet and sour taste when eaten. The *A. bunius* fruit is traditionally used as a therapeutic remedy for gastrointestinal problems, diabetes and hypertension [1]. The fruit has been widely used for the making of jam, juice concentrate and wine. The antioxidant and pharmacological activities of the bioactive compounds derived from

this fruit, such as polyphenols and flavonoids, are documented in the literature [1-3].

Colorectal cancer (CRC) is the third most common cancer worldwide [4]. CRC usually begins with a non-cancerous proliferation of mucosal epithelial cells of the large intestine [5]. Uncontrolled replication and survival of these cells result in the formation of benign adenoma (also known as polyps), which upon acquiring a series of genetic or epigenetic aberrations, may develop into carcinoma and metastasize [5].

While the clinical and genetic understanding of the pathogenesis of CRC has increased over the years, the

molecular etiology of this disease beyond the initial carcinogenesis cascade remains poorly understood. Oxidative stress has long been implicated in the pathophysiology of cancers, suggesting that antioxidant treatment could afford a degree of protection from the cellular carcinogenic cascade of events. However, cancer cells have developed an adaptive advantage to resist reactive oxygen species (ROS) without compromising their metabolic demands while avoiding oxidative damage [6]. Mitochondria, being the site of oxidative phosphorylation, are the major source of ROS [7]. Several lines of evidence suggest that oxidative stress, as a consequence of mitochondrial dysfunction, is one of the major drivers of carcinogenesis [8].

In cancer biology, autophagy has been shown to play dual roles in tumor promotion and suppression [9]. Autophagy is a tightly regulated intracellular self-degradative process for the removal and recycling of damaged cytoplasmic materials. Cells use autophagy to maintain cellular homeostasis or as an adaptive response to cellular starvation, development and death [9]. As cancer cells have high metabolic requirements, it is likely that selective autophagy of the mitochondria, a molecular process known as mitophagy, may be induced to meet these demands [10].

Neoadjuvant chemotherapy is the standard treatment for CRC patients with metastatic progression [5]. However, its cytotoxicity, along with the emergence of drug resistance and recurrence of cancer, has hindered its success in some patients [5]. Plant-based treatment for cancer has received much attention in recent years as an inexpensive alternative to cytotoxic chemotherapy. Despite the plethora of reports on the phytochemical content and biological activities of *A. bunius* fruit, its anticancer properties remain underexplored.

In the present study, the total phenolic and flavonoid content, as well as the radical scavenging activity of *A. bunius* fruit aqueous crude extract (ACE) were determined. The effects of *A. bunius* ACE on the viability, redox status and mitochondrial integrity were investigated using a human-derived colorectal cell line, HCT 116. To gain further insight into the anticancer activity of *A. bunius*, its effects on the expression of key genes associated with oxidative stress and autophagy were also examined.

MATERIALS AND METHODS

Preparation of *A. bunius* fruit aqueous extracts

A. bunius fruits were harvested from Sucat, Paranaque City, Philippines (14.4618° N, 121.0254° E). Ripe fruits were carefully selected and thoroughly washed with distilled water. The fruits were deseeded and lyophilized using a freeze dryer (Labconco, Kansas City, MO, USA). The lyophilized samples were ground into a fine powder using a mechanical blender. Samples were separately heated at 60°C, 100°C and 150°C for 30 min in a convection oven. Aqueous extraction was performed by adding 40 mL H₂O to 2.0 g of sample followed by constant stirring overnight at room temperature. The extracts were vacuum-filtered using Whatman no. 1; the filtrate was then filtered using a 0.22- μ m syringe filter (Merck Millipore, Burlington, MA, USA). The filtrate was stored at -25°C and protected from light until further analysis. All reagents were purchased from Sigma-Aldrich (St. Louis, MO, USA) unless otherwise stated.

Total phenolic content (TPC)

TPC was determined as described previously [11], with slight modifications. One hundred μ L of *A. bunius* ACE (5 mg/mL) was mixed with 750 μ L of Folin-Ciocalteu reagent and incubated for 5 min. To the mixture, 750 μ L of 7% sodium carbonate was added and incubated for 90 min in the dark. The absorbance of samples was measured at 795 nm using a UV-visible spectrophotometer (Hitachi, Tokyo, Japan). Gallic acid was used as a standard. TPC was expressed as mg gallic acid equivalence (GAE) per g of freeze-dried sample.

Total flavonoid content (TFC)

TFC was determined as described previously [12], with slight modifications. Five hundred μ L of *A. bunius* ACE (5 mg/mL) was mixed with 550 μ L of deionized H₂O and 150 μ L of sodium nitrite, followed by incubation for 5 min. Three hundred μ L of 10% aluminum chloride hexahydrate was then added to the mixture. The sample was mixed for 5 min followed by the addition of 1 mL of 1 M of sodium hydroxide. The absorbance of samples was measured at 420 nm using a UV-visible spectrophotometer (Hitachi, Tokyo,

Japan). Quercetin was used as a standard. TFC was expressed as mg quercetin equivalence (QE) per g of freeze-dried sample.

Radical scavenging activity (RSA)

The RSA was determined as described previously [13], with slight modifications. Five hundred μL of *A. bunius* ACE (5 mg/mL) was mixed with 2 mL of 0.1 M 2,2-diphenyl-1-picrylhydrazyl (DPPH). The sample was vortex-mixed for 30 s and incubated for 30 min in the dark. The absorbance of samples was measured at 517 nm using a UV-visible spectrophotometer. Tocopheryl acetate was used as positive control. RSA was expressed as percent RSA (%RSA) relative to solvent blank.

Cell culture

The HCT 116, HepG2 (human liver cancer cell line) and THLE-3 (human normal liver epithelial cell line) were cultured in Dulbecco's modified Eagle's medium/Ham's F-12 medium (DMEM/F-12) with GlutaMAX (Invitrogen, Carlsbad, CA, USA) supplemented with 10% fetal bovine serum (Invitrogen, Carlsbad, CA, USA) and 100 U/mL penicillin/100 $\mu\text{g}/\text{mL}$ streptomycin (Invitrogen, Carlsbad, CA, USA). For THLE2 cells, 1 $\mu\text{g}/\text{mL}$ of recombinant human epidermal growth factor (ImmunoTools, Friesoythe, Germany) was added to the culture medium. Cells were grown in a humidified atmosphere with 5% CO_2 at 37°C.

Cell treatment

Cells were seeded in a 25-cm² tissue culture flask and grown to 80% confluence. Prior to treatment, the cells were washed with pre-warmed phosphate-buffered saline (PBS) and treated with *A. bunius* ACE to final concentrations of 0.037, 0.11, 0.33 and 1.0 mg/mL in 0.1% dimethyl sulfoxide (DMSO) for 48 h. Complete culture medium with 0.1% DMSO was used as a vehicle control (VC).

Resazurin assay

Five thousand cells were seeded into a 96-well, black, clear-bottom tissue culture plate (4titude, Surrey, UK) and grown to 60-80% confluence. The cells were treated with *A. bunius* extract (0-50 mg/mL in 0.1% DMSO).

The cells were washed twice with pre-warmed PBS and incubated with 0.05% resazurin at 37°C for 90 min. Cell viability was assessed by measuring the metabolic capacity of cells in reducing resazurin to a highly fluorescent compound, resorufin. The fluorescence of resorufin was measured using a scanning fluorescence microplate reader (BMG Labtech, Ortenberg, Germany) with the excitation and emission wavelength set to 530 nm and 590 nm, respectively. The lethal concentration 50 (LC_{50} , the concentration required to kill 50% of the cell population) was determined using the GraphPad Prism 6.0 software (GraphPad, San Diego, CA, USA).

Trypan blue assay

About 1×10^6 cells/mL of cells were seeded in a 25-cm² tissue culture flask and grown to 80% confluence. The cells were washed with PBS twice and incubated with 0.25% trypsin-EDTA at 37°C for 5 min to facilitate cell detachment. One hundred μL of cell suspension were stained with 100 μL 0.1% trypan blue. The cell suspension was loaded into a hemocytometer and viewed under an inverted phase-contrast microscope (Nikon, Tokyo, Japan). Cell viability was assessed by counting the stained cells (dead cells) on at least 4 fields of view; 100 μM of hydrogen peroxide (H_2O_2) served as a positive control.

Cell morphology analysis

Cells were seeded in 6-well tissue culture plate and grown to 80% confluence. The morphology of the cells was visualized using an inverted phase-contrast microscope (Nikon, Tokyo, Japan) at 100 \times , 200 \times and 400 \times magnification. At least 5 fields of view were collected for morphological analysis. Images were analyzed using the NIS Elements Viewer Software (Nikon, Tokyo, Japan); 100 μM of hydrogen peroxide (H_2O_2) served as a positive control.

General oxidative stress index

Cells were seeded in a 96-well black, clear-bottom microplate and were grown to 80% confluence. The cells were incubated with a redox-sensitive fluorogenic dye, 2',7'-dichlorodihydrofluorescein diacetate (H_2DCFDA) (Invitrogen, Carlsbad, CA, USA) (10 μM) for 45 min at 37°C. The cells were washed twice with PBS and

incubated with serum-free DMEM for an additional 30 min. The DCF fluorescence ($\lambda_{\text{ex}}=485/12$; $\lambda_{\text{em}}=520$) was measured using a microplate reader (BMG Labtech, Ortenberg, Germany). Cells incubated with H_2O_2 (100 μM) served as a positive control. Since the oxidation of DCF not only depends on the intracellular ROS content but also on the overall cellular antioxidant capacity [14], the DCF fluorescence intensity was interpreted as the intracellular general oxidative stress index.

Total glutathione (GSH) assay

Cells were washed twice with ice-cold PBS and lysed using ice-cold lysis buffer (0.1% Triton-X and 0.6% sulfosalicylic acid in 0.1 M sodium phosphate buffer (Na-PB), pH 7.4). The cell lysates were vortex-mixed for 3 min and centrifuged at $3000 \times g$ for 4 min at 4°C . Twenty μL of the supernatant were placed in a 96-well clear microplate and were mixed with 100 μL of reaction mixture containing: 0.15 mM 5,5'-dithiobis-2-nitrobenzoic acid, 0.2 mM reduced nicotinamide adenine dinucleotide phosphate (NADPH) and 1.0 U/mL glutathione reductase, in 0.1 M Na-PB, pH 7.4. The absorbance of the samples was measured at 412 nm with 30 s read intervals for 12 cycles using a scanning microplate reader (BMG Labtech, Ortenberg, Germany). The concentration of GSH was calculated against a standard curve prepared from GSH solutions of known concentrations (0-0.28 mM). The precipitate was set aside for the protein assay. The total GSH concentration was normalized for the protein content of lysates.

Bradford assay

The protein content of samples was determined by the Bradford assay. In brief, the precipitate was dissolved with 500 μL of 0.5 M sodium hydroxide. Five μL of the sample were placed in a clear 96-well clear microplate and mixed with 200 μL of Bradford reagent. The absorbance of the samples was measured at 595 nm using a microplate reader (BMG Labtech, Ortenberg, Germany). The protein concentration was determined against a standard curve prepared from bovine serum albumin (20-1000 $\mu\text{g}/\text{mL}$).

Mitochondrial transmembrane potential (MTP)

Cells (50000) were seeded in a 96-well black, clear-bottom tissue culture microplate and grown to 80% confluence. The cells were incubated with 2 μM of MTP-sensitive dye, JC-1 (Invitrogen) for 30 min at 37°C . At high MTP, JC-1 spontaneously forms J-aggregates that emit an intense red fluorescence. At low MTP, JC-1 remains in the monomeric form that has a green fluorescence. The fluorescence of J-aggregates ($\lambda_{\text{ex}}=485/12$; $\lambda_{\text{em}}=590/10$) and J-monomers ($\lambda_{\text{ex}}=485/12$; $\lambda_{\text{em}}=520$) were measured using a fluorescence microplate reader (BMG Labtech, Germany). The MTP was assessed by obtaining the ratio between the red and green fluorescence; 100 μM of H_2O_2 served as a positive control.

Quantitative polymerase chain reaction (qPCR)

Quantitative polymerase chain reaction (qPCR)

RNA was extracted from cells using the TRIreagent (Bioline, Memphis, TN, USA) following the manufacturer's protocol, with slight modifications. cDNA synthesis was performed using the SensiFAST cDNA Synthesis Kit (Bioline, London, UK) according to the manufacturer's protocol. The cDNA was then used as the template for qPCR using SensiFAST™ SYBR® Hi-ROX kit (Bioline) following the manufacturer's protocol, with slight modifications, using the RotoGene Q real-time PCR machine (QIAGEN, Antwerp, Belgium). The following primer sequences were used for qPCR analysis: *BECLIN-1* (forward, 5'-ATGCAGGTGAGCTTCGTGTG-3'/ reverse, 5'-CTGGGCTGTGGTAAGTAATGGA-3'); *ATG5* (forward, 5'-GCTATTGATCCTGAAGATGGGG-3'/ reverse, 5'-CTTGCAGCAGCGAAGTGTTT-3'); *LC3* (forward, 5'-TAATTAGAAGGCGCTTACAGCTCA-3'/ reverse, 5'-TGAAGGTCTATTTTATGGCAACTT-3'); *NRF2* (forward, 5'-GTGGATCTGCCAACTACTCCC-3'/ reverse, 5'-AAACGTAGCCGAAGAAACCTCA-3'); *GPX1* (forward, 5'-AGTCGGTGTATGCCTTCTCG-3'/ reverse, 5'-TCTTGGCGTTCTCCTGATGC-3'); *TRXR1* (forward, 5'-GGTGATGGTCTGACTTTGTC-3'/ reverse, 5'-TGCTTAACTGTCTCCTCGACT-3'). The expression levels of gene targets were determined using the comparative cycle threshold ($\Delta\Delta C_T$) method with β -actin as an endogenous control.

Statistical analyses

All measurements were done in at least triplicate, and at least in three independent experiments. The data were reported as the mean±standard deviation (SD). Data sets with three or more groups were analyzed by analysis of variance (ANOVA) using Dunnett's multiple comparisons test as the *post hoc* test. Unpaired *t*-test was performed to test for statistical significance between two groups. A *p* value of ≤0.05 was considered statistically significant. All statistical analysis was performed using the GraphPad Prism 6.0 software (GraphPad, San Diego, CA, USA).

RESULTS

Thermal treatment of lyophilized *A. bunius* fruits did not improve its TPC and TFC

Preliminary experiments were performed to determine if thermal treatment of lyophilized *A. bunius* fruits prior to aqueous extraction influences its TPC and TFC. The TPC did not differ significantly when *A. bunius* fruit was heated at 60°C and 100°C (*p*=0.802 and *p*=0.789, respectively) (Fig. 1A). A slight but

significant reduction in TPC was observed when the samples were heated at 150°C compared to room temperature (8.6 ± 0.3 vs 9.7 ± 0.6 mg GAE/g sample, respectively, *P*<0.05).

A similar trend was observed for TFC as heating of *A. bunius* fruit samples at 60°C and 100°C did not produce significant changes (*P*=0.976 and *P*=0.363, respectively) (Fig. 1B). However, heating the samples at 150°C resulted in a reduction in TFC compared with room temperature (15.8 ± 0.2 vs 18.2 ± 0.1 mg QE/g sample, respectively, *P*<0.05).

The percentage of RSA remained unchanged when *A. bunius* fruit samples were heated at 60°C (*P*=0.995), but slightly increased at 100°C compared to room temperature (66.2 ± 1.4 vs $59.3\pm 2.0\%$ RSA, respectively, *P*<0.001) (Fig. 1C). A marked reduction in the percentage of RSA was observed when the samples were heated at 150°C compared to room temperature (49.6 ± 1.4 vs $59.3\pm 2.0\%$ RSA, respectively, *P*<0.001).

Since the TPC, TFC and the %RSA were unaffected by the thermal treatment, subsequent experiments were performed using *A. bunius* ACE obtained from lyophilized *A. bunius* fruits maintained at room temperature prior to aqueous extraction.

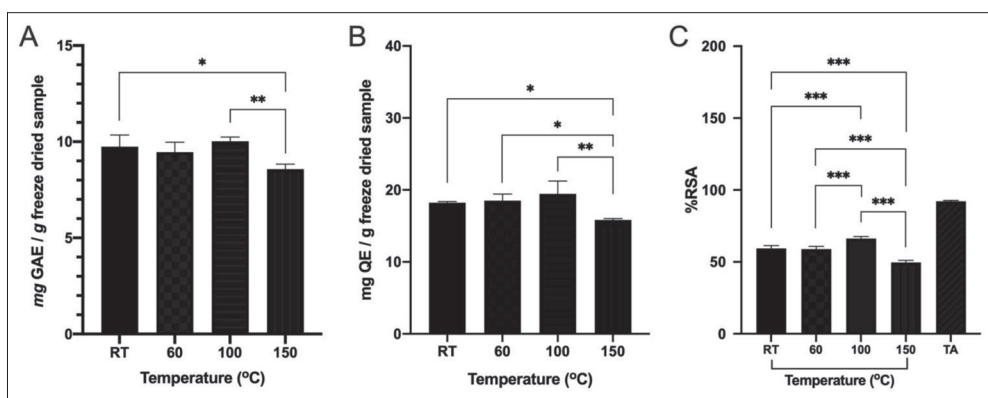


Fig. 1. Total phenolic content (TPC), total flavonoid content (TFC) and radical scavenging activity (RSA) of *A. bunius* ACE. Lyophilized *A. bunius* fruit samples were separately heated at 60°C, 100°C and 150°C prior to aqueous extraction. A separate sample was kept at room temperature as a reference. The TPC of *A. bunius* ACE was determined spectrophotometrically using the Folin-Ciocalteu reagent. Results were expressed as the mean mg GAE/g freeze-dried sample±SD (A). The TFC of *A. bunius* ACE was determined spectrophotometrically based on the complexation of aluminum ion with the hydroxyl and carbonyl groups of flavonoid compounds. Results were expressed as mean mg QE/g freeze-dried sample±SD (B). The RSA of *A. bunius* ACE was determined spectrophotometrically using the DPPH reagent. Results were expressed as the mean %RSA±SD (C). *, **, and *** indicate statistically significant differences at *P*<0.05, *P*<0.01 and *P*<0.001, respectively. GAE – gallic acid equivalent; QE – quercetin equivalent; RT – room temperature; TA – tocopherol acetate

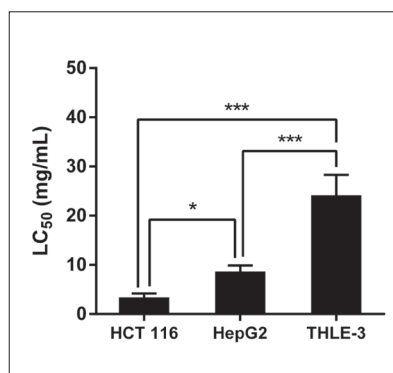


Fig. 2. Cytotoxicity of *A. bunius* ACE on cancer and normal cell lines. HCT 116, HepG2 and THLE-3 cells were treated with *A. bunius* ACE (0-50 mg/mL) for 48 h. The toxicity of *A. bunius* was determined by measuring the metabolic capacity of the cells in reducing resazurin to a highly fluorescent compound, resorufin. The LC₅₀ was calculated for each cell line. The results were expressed as the mean ± SD of three independent experiments. * and *** indicate statistical significant difference at $P < 0.01$ and $P < 0.001$, respectively. *A. bunius* ACE – *Antidesma bunius* aqueous crude extract; LC₅₀ – 50% lethal concentration.

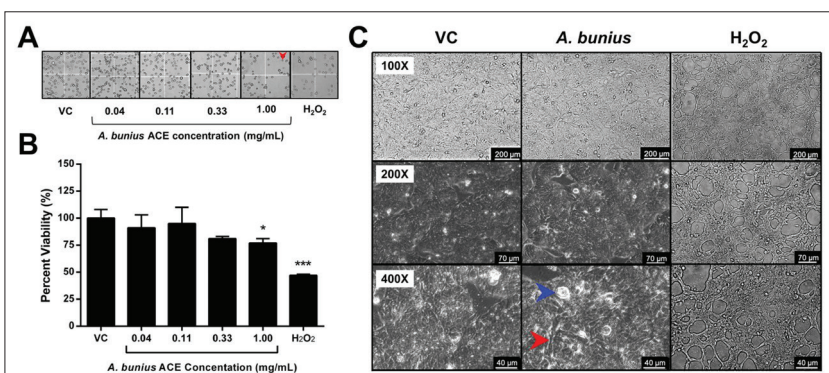


Fig. 3. Effects of *A. bunius* ACE on the viability and morphology of HCT 116 cells. HCT 116 cells were treated with increasing concentrations of *A. bunius* ACE for 48 h. Cell viability was assessed by the trypan blue assay. Using a hemocytometer, the viable (unstained) and dead (stained) cells (red arrow) were counted in at least three fields of view under a phase-contrast microscope (A). Cell viability was expressed as the mean percent viability ± SD of three independent experiments (B). Cell morphology was assessed using a phase-contrast microscope at 100×, 200×, 400× magnification (C). Blue arrow – apoptotic bodies; red arrow – dead (stained) cells. One hundred μM hydrogen peroxide (H₂O₂) served as a positive control. The red arrow indicates epithelial cobblestone morphology and blue arrow indicates apoptotic bodies. * indicates statistically significant difference at $P < 0.05$. *A. bunius* ACE, *Antidesma bunius* aqueous crude extract; VC, vehicle control

A. bunius ACE exhibited the highest toxicity in colorectal cancer cells

The resazurin assay was performed to determine the cytotoxicity of *A. bunius* extract. HCT 116 had a LC₅₀ of 3.4 ± 0.8 mg/mL (Fig. 2); HepG2 had a higher LC₅₀ (8.7 ± 1.2 mg/mL, $p < 0.01$) than HCT 116; in comparison, THLE-3 cells recorded a 7-fold higher LC₅₀ (24.2 ± 4.1 mg/mL, $P < 0.001$) than HCT 116. The results indicate that *A. bunius* is more toxic to cancer cells than to normal cells. Notably, *A. bunius* exhibited the highest toxicity in colorectal cancer cells at a relatively low concentration. Hence, subsequent experiments focused on the effects of *A. bunius* on HCT 116 cells.

A. bunius ACE induced cell death and morphological alterations in colorectal cancer cells

Among the concentrations that were tested, 1.0 mg/mL of *A. bunius* ACE resulted in a reduction in viability of HCT-116 cells by ~27% ($P < 0.05$) (Fig. 3A and B). This concentration was considered a sublethal concentra-

tion and was used in subsequent experiments to avoid direct toxicity due to the use of a high concentration of *A. bunius* ACE.

Cells treated with *A. bunius* ACE exhibited intact tight junctions and an improved cobblestone phenotype (Fig. 3C, red arrow), while VC-treated cells displayed partial loss of cobblestone morphology. Apoptotic bodies were more frequently observed on *A. bunius* ACE-treated cells (Fig. 3C, blue arrow) compared with VC-treated cells. In addition, VC-treated cells were homogeneously distributed on a cultured field, exhibiting a uniform polygonal shape (Fig. 3C). Conversely, *A. bunius* ACE-treated cells exhibited elongation and a spindle-like phenotype.

A. bunius ACE reduced oxidative stress and increased the expression of redox-sensitive genes in colorectal cancer cells

To determine the antioxidant capacity of *A. bunius* ACE and its effects on the general oxidative stress index of CRC cells, cells were probed with a redox-sensitive

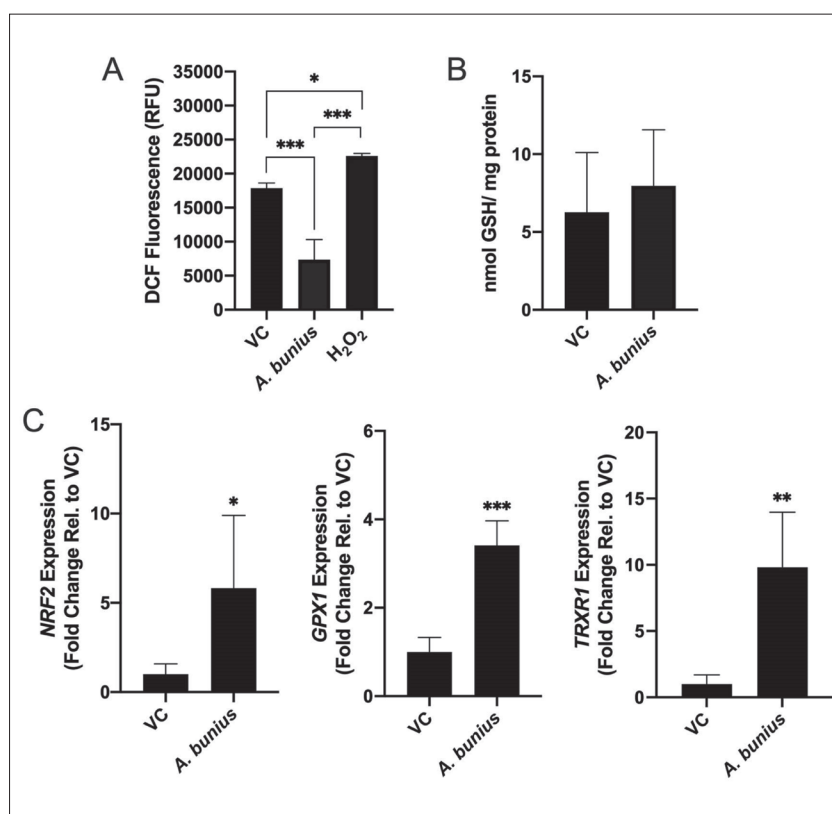


Fig. 4. Effects of *A. bunius* ACE on the redox status and expression of redox-sensitive genes in HCT 116 cells. HCT 116 cells were treated with *A. bunius* ACE (1 mg/mL) for 48 h. The general oxidative stress index of cells was assessed using the redox-sensitive dye, H₂DCFDA. The DCF fluorescence was measured using a fluorescent microplate reader. One hundred μ M hydrogen peroxide (H₂O₂) served as a positive control. The results are expressed as DCF relative fluorescence units \pm SD of three independent experiments (A). Total GSH levels were measured using the enzyme recycling assay. The GSH content was expressed as μ g GSH/mg protein \pm SD of three independent experiments (B). The expression of *NRF2*, *GPX1*, and *TRXR1* genes was measured using qPCR. The results were expressed as the -fold change relative (Rel.) to vehicle control (VC) \pm SD of three independent experiments (C). *, **, and *** indicate statistically significant difference at $P < 0.05$, $P < 0.01$, and $P < 0.001$, respectively. *A. bunius* ACE – *Antidesma bunius* aqueous crude extract; DCF – dichlorofluorescein; GSH – glutathione; *NRF2* – nuclear factor erythroid 2-related factor 2; *GPX1* – glutathione peroxidase 1; *TRXR1* – thioredoxin reductase 1.

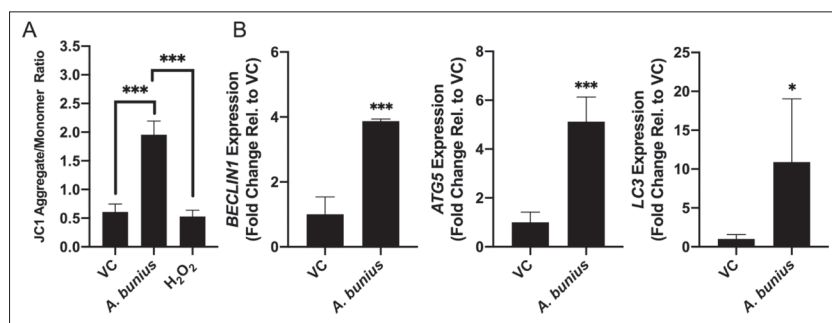


Fig. 5. The effects of *A. bunius* ACE on mitochondrial integrity and expression of autophagy-associated genes in HCT 116 cells. HCT 116 cells were treated with *A. bunius* ACE (1 mg/mL) for 48 h. The mitochondrial transmembrane potential (MTP) of cells was assessed using the JC-1 dye. The fluorescence of JC-1 aggregates (high MTP) and monomers (low MTP) were measured simultaneously using a fluorescence microplate reader. One hundred μ M hydrogen peroxide (H₂O₂) served as a positive control. The results are expressed as the ratio of J-aggregates/J-monomers \pm SD of three independent experiments (A). The expression of *BECLIN1*, *ATG5* and *LC3* genes was measured using qPCR. The results were expressed as the -fold change relative (Rel.) to vehicle control (VC) \pm SD of three independent experiments (B). * and *** indicate statistically significant difference at $P < 0.05$ and $P < 0.001$, respectively. *A. bunius* ACE – *Antidesma bunius* aqueous crude extract; *BECLIN1* – coiled-coil myosin-like BCL2-interacting protein gene; *ATG5* – autophagy related 5 protein gene; *LC3* – microtubule-associated protein 1A/1B-light chain 3 gene.

dye, H₂DCF-DA. *A. bunius* ACE-treated cells exhibited a lower DCF fluorescence than VC-treated cells (7379 \pm 2940 relative fluorescence units vs 17871 \pm 746 SD, $P < 0.01$) (Fig. 4A), which indicates a reduction in intracellular oxidative stress.

GSH is the most abundant redox buffer and antioxidant in mammalian cells. Changes in GSH levels can be the consequence of the exposure of cells to an oxidative insult or to fluctuations in thiol availability. Despite the reduction in intracellular oxidative stress index, the total GSH in *A. bunius* ACE-treated cells remained unaltered (Fig. 4B, $P = 0.925$).

NRF2 is an important stress-responsive transcription factor, especially during oxidative stress.

Treatment of cells with *A. bunius* ACE resulted in a marked 6-fold ($P<0.05$) increase in *NRF2* expression as compared to VC-treated cells (Fig. 4C). This was accompanied by an increase in the expression of *NRF2*-dependent genes, *GPX1* (3-fold, $P<0.001$) and *TRX1* (10-fold, $P<0.01$).

***A. bunius* ACE increased the mitochondrial transmembrane potential and enhanced the expression of autophagy-associated genes in colorectal cancer cells**

To assess whether *A. bunius* ACE can influence the mitochondrial integrity of CRC cells, *A. bunius* ACE-treated cells were incubated with a MTP-sensitive dye, JC-1. *A. bunius* ACE-treated cells displayed a higher J-aggregate/J-monomer ratio when compared to VC-treated cells (1.96 ± 0.24 SD vs 0.61 ± 0.14 SD, respectively, $P<0.001$) (Fig. 5A). This result indicates that *A. bunius* ACE improves the MTP in CRC cells.

The autophagy canonical pathway involves the assembly of key proteins, BECLIN1, ATG5 and LC3, for the formation of autophagosomes. Interestingly, a marked increase in the expression of *BECLIN1* (4-fold, $P<0.001$), *ATG5* (5-fold, $P<0.001$) and *LC3* (11-fold, $P<0.01$) genes was observed in *A. bunius* ACE-treated cells (Fig. 5B), which suggests that *A. bunius* ACE promotes the induction of autophagy in CRC cells.

DISCUSSION

Chemotherapy is the standard treatment for metastatic CRC. However, its non-specific cytotoxicity remains a major drawback as it also causes serious damage to healthy cells. The use of plant-derived extracts has historically been part of treatment of different diseases, including cancer. *A. bunius* fruit is a promising herbal therapy for cancer as it has been previously shown to possess antioxidant, antiinflammatory and antimutagenic activities [1,3]. However, the paucity of definitive and conclusive data on its mechanism of action impedes the use of this fruit as an adjunct treatment for cancer.

Research interest on phenolic and flavonoid compounds comes from their therapeutic potential against oxidative damage associated with different diseases,

including cancer. The phytochemical content of *A. bunius* was extensively reported in the literature, with the majority of studies using alcoholic solvents such as ethanol and methanol because of their high polarity and ability to effectively solubilize many phenolic and flavonoid species [3,13]. Very few studies employed aqueous extractions of *A. bunius* fruits since water and water-based solvents are regarded as inferior to alcohol-based extraction in terms of phytochemical yield. However, aqueous extraction offers several advantages over conventional solvent extraction; it does not use toxic chemicals, it is environmentally friendly in terms of solvent and energy consumption, and it can be streamlined for the production of herbal products or functional foods that are suitable for human consumption [15]. In the present study, the TPC of *A. bunius* ACE yielded comparable results with the previously reported studies in *A. bunius* fruits that used aqueous methanol as an extraction solvent [16,17]. These observations suggest that aqueous extraction may be equally effective as alcohol-based extraction in extracting phenolic compounds from lyophilized *A. bunius* fruits. We hypothesized that the loss of water during lyophilization could have allowed for the reduction and polymerization of polyphenols, thus increasing their concentration in dehydrated samples [18].

A plethora of studies have demonstrated various pharmacological activities of flavonoids such as anti-inflammatory, antidiabetic, anti-aging and anticancer activities [19]. Interestingly, *A. bunius* yielded one of the highest TFCs among locally available selected fruits in the Philippines [17]. In the present study, the TFC of *A. bunius* ACE was within the range previously reported for *A. bunius* fruits using aqueous methanol as an extraction solvent [20].

Heat treatment was previously demonstrated to increase the availability of phenolics and flavonoids in certain fruits [21,22]. Presumably, the insoluble, bound phenolics and flavonoids can be released from the cell wall during the heating, boiling or roasting processes [23]. We demonstrated that heat treatment of lyophilized *A. bunius* fruits up to 100°C had no effects on the TPC and TFC, while a considerable reduction in TPC and TFC was observed at 150°C. This trend was also reflected in the %RSA, which showed no change at 60°C and only a minimal increase at 100°C. Our results suggest that the phenolic and flavonoid compounds

in *A. bunius* fruits are predominantly soluble, in an unbound form, and hence, they were susceptible to thermal degradation.

The primary goal of cancer chemotherapy is to specifically target cancer cells without exhibiting toxicity to healthy cells. This is one of the major challenges in the use of several chemotherapeutic agents; hence, selective toxicity must be a paramount consideration in the discovery of leads for cancer treatment. Among the cell lines that were tested, *A. bunius* exhibited the highest toxicity in cancer cells, with the most profound effects in HCT 116 cells. Thus, *A. bunius* may have a potential selective toxicity to cancer cells. A relatively low dose of *A. bunius* ACE (1 mg/mL) induced appreciable cell death by ~27% in HCT 116 cells. At this sublethal concentration, *A. bunius* ACE could have possibly induced a hormetic effect in HCT 116 cells [24]. Hormesis is characterized by a biphasic response to the exposure to increasing concentrations of a particular chemical compound, where a low concentration generally produces a favorable response [25]. Hence, even a relatively low concentration of *A. bunius* ACE stimulated specific molecular alterations in cancer cells while a higher concentration resulted in non-specific cytotoxic effects. This also suggests that a low concentration of *A. bunius* has the potential to produce beneficial effects with negligible cytotoxic effects to normal cells. It was previously shown that a low-dose treatment strategy for cancer therapy may be equally beneficial as a conventional-dose treatment but with decreased toxicity [26]. In a recent study, the effects *A. bunius* aerial parts were investigated in different cancer cell lines [2]. Consistent with our observation, the water-soluble fraction of *A. bunius* was shown to be cytotoxic against MCF7 and HepG2 cell lines.

Notably, *A. bunius* ACE augmented the tight junction structure in HCT 116 cells. Consistent with our observations, some plant-derived compounds such as quercetin and berberine have been shown to improve the tight junction barrier function of the intestinal epithelium [27]. Tight junctions in epithelial cells provide a physical barrier and are important for cell signaling and paracellular movement of substances. Their loss has also been implicated in tumor cell mobility and invasiveness [28]. Therefore, *A. bunius* ACE may promote the arrest of cancer cell migration and invasiveness by altering the tumor cell microenvironment.

The involvement of oxidative stress in the etiology of cancer is extensively documented in the literature [29]. Oxidative stress is characterized by the uncontrolled intracellular production of ROS combined with insufficient antioxidant defenses [30]. In the present study, we observed that *A. bunius* ACE treatment improved antioxidant activity by reducing the oxidative stress index in HCT-116 cells, coupled with the upregulation of *NRF2* and *NRF2*-dependent antioxidant genes, *GPX1* and *TRX1*. *NRF2* is a universal stress-responsive transcription factor that binds to antioxidant response elements, which in turn regulate the expression of downstream antioxidant genes such as *GPX1* and *TRXR1* to counteract the oxidative insult [31]. We hypothesized that the upregulation of *NRF2* and *NRF2*-dependent genes points to the activation of antioxidant defenses in HCT 116 cells in response to *A. bunius* ACE, which may also partly explain the reduction in oxidative stress. Studies have demonstrated a decline in ROS in response to exposure to plant-derived extracts and/or antioxidants. Most recently, luteolin, a type of flavonoid, was found to promote apoptotic cell death via upregulation of *NRF2* in HCT 116 cells [32,33]. Luteolin was also found to reduce the intracellular ROS content in HT-29 and SNU-407 cancer cell lines [33]. Interestingly, luteolin was also identified in *A. bunius* fruit extracts [16]. Despite the observed changes in the oxidative stress index of HCT 116 cells, total GSH levels were unperturbed by *A. bunius* ACE. GSH is essential in supporting the activity of *GPX1* and counteracting oxidative stress in HCT 116 cells. However, further studies on GSH metabolism are warranted to establish the role of GSH in the overall redox status of colon cancer cells. Cancer cells can adapt to an oxidizing environment and have increased demands for ROS to support their rapid proliferation rate [6]. Our results suggest that *A. bunius* ACE modulates the redox status in colon cancer cells by depriving these cells of ROS. This may represent a novel mechanism by which phytochemicals in *A. bunius* fruits prevent cellular transformation and tumorigenesis and promote the demise of cancer cells.

Mitochondria are widely considered as important sources of intracellular ROS through oxidative phosphorylation. This makes mitochondria the main targets of regulatory and toxic actions of ROS that can influence the cell cycle, cell proliferation and apoptosis [7]. We have observed an increase in the MTM potential in

HCT 116 cells following treatment with *A. bunius* ACE. This effect may have prevented the leakage of ROS from the mitochondrial compartment and could explain, at least in part, the reduction in the general oxidative stress index in *A. bunius* ACE-treated HCT 116 cells.

The increase in the MTP of HCT 116 cells also suggests that *A. bunius* ACE promotes mitochondrial quality control, which could influence the removal of low-potential mitochondria. However, it is not clear how this phenomenon signals apoptotic death in cancer cells. Autophagy is a molecular process that facilitates the timely elimination of dysfunctional mitochondria and is essential in protecting cells from a disordered mitochondrial metabolism and ROS leakage. *A. bunius* ACE treatment resulted in the upregulation of key genes involved in autophagy, which indicates induction of autophagy. Since dysfunctional mitochondria serve as a signal for malignant transformation of healthy cells [8], we hypothesized that the activation of autophagy by *A. bunius* ACE is an upstream event that mediated the clearance of damaged mitochondria and helped in preventing ROS leakage [10]. Indeed, increased MTM potential and decreased oxidative stress were both observed following treatment with *A. bunius* ACE. The relationship between autophagy and apoptosis in cancer has been demonstrated in various studies, and it has been suggested that autophagy may function as a protective mechanism that arrests uncontrolled cell growth, which is associated with cancer [34]. In agreement with this, studies have shown that several pathways related to autophagy are downregulated during malignant transformation [9,10,34]. It has also been proposed that mitochondria play a central role in the crosstalk between autophagy and apoptosis [34]. Depolarized mitochondria is an upstream signal for the activation of autophagy in an attempt to segregate dysfunctional mitochondria from healthy ones [34]. Therefore, our results suggest that the modulation of autophagy by the phytoconstituents in *A. bunius* could have favored mitochondrial repair and improvement of the redox status in CRC cells. These alterations may represent part of a cascade of events that lead to the blocking of malignant growth and commitment of colorectal cancer cells to cell death. However, the results described in the present study only provide preliminary insight into the anticancer activity of *A. bunius*. Therefore, further investigations are warranted on other key molecular players that orchestrate the

crosstalk between autophagy and apoptotic-related pathways, which should be beneficial in shedding further light into the anticancer mechanism effected by *A. bunius*.

Funding: This study was supported by the De La Salle University Research Fellowship Program.

Acknowledgements: We gratefully acknowledge the De La Salle University for the funding this study, and members of the Sumayao Research Group for their technical assistance and scientific discussions.

Author contributions: SB and JLL performed the experiments and contributed during preparation of the manuscript. RS prepared the study design, assisted in the interpretation of the results and contributed to the preparation of the manuscript. GO assisted in the conduct of experiments and contributed to the technical discussions and the interpretation of the results.

Conflict of interest disclosure: None declared.

REFERENCES

1. Islam S, Koly S. A review on phytochemical and pharmacological potentials of *Antidesma bunius*. *J Anal Pharm Res.* 2018;7:602-4.
2. Ibrahim TA, El Dib RA, Al-Youssef HM, Amina M. Chemical composition and antimicrobial and cytotoxic activities of *Antidesma abunius* L. *Pak J Pharm Sci.* 2019;32(1):153-63.
3. Jorjong S, Butkhup L, Samappito S. Phytochemicals and antioxidant capacities of Mao-Luang (*Antidesma bunius* L.) cultivars from Northeastern Thailand. *Food Chem.* 2015;181:248-55.
4. Bray F, Ferlay J, Soerjomataram I, Siegel RL, Torre LA, Jemal A. Global cancer statistics 2018: GLOBOCAN estimates of incidence and mortality worldwide for 36 cancers in 185 countries. *CA Cancer J Clin.* 2018;68(6):394-424.
5. Rawla P, Sunkara T, Barsouk A. Epidemiology of colorectal cancer: Incidence, mortality, survival, and risk factors. *Prz Gastroenterol.* 2019;14(2):89.
6. Sosa V, Moliné T, Somoza R, Paciucci R, Kondoh H, LLeonart ME. Oxidative stress and cancer: an overview. *Ageing Res Rev.* 2013;12(1):376-90.
7. Cadenas E. Mitochondrial free radical production and cell signaling. *Mol Aspects Med.* 2004;25(1-2):17-26.
8. Porporato PE, Filigheddu N, Bravo-San Pedro JM, Kroemer G, Galluzzi L. Mitochondrial metabolism and cancer. *Cell Res.* 2018;28(3):265-80.
9. Yun CW, Lee SH. The roles of autophagy in cancer. *Int J Mol Sci.* 2018;19(11):3466.
10. Vara-Perez M, Felipe-Abrio B, Agostinis P. Mitophagy in Cancer: A Tale of Adaptation. *Cells.* 2019;8(5):493.
11. Bakar A, Fadzelly M, Ismail NA, Isha A, Ling M, Lee A. Phytochemical composition and biological activities of selected wild berries (*Rubus moluccanus* L., *R. fraxinifolius* Poir., and *R. alpestris* Blume). *Evid Based Complement Alternat Med.* 2016;2016:2482930.

12. Ghasemzadeh A, Jaafar HZ, Rahmat A. Antioxidant activities, total phenolics and flavonoids content in two varieties of Malaysia young ginger (*Zingiber officinale* Roscoe). *Molecules*. 2010;15(6):4324-33.
13. Drózdź P, Šežienė V, Pырzynska K. Phytochemical properties and antioxidant activities of extracts from wild blueberries and lingonberries. *Plant Foods Hum Nutr*. 2017;72(4):360-4.
14. Jakubowski W, Bartosz G. 2, 7-dichlorofluorescein oxidation and reactive oxygen species: what does it measure? *Cell Biol Int*. 2000;24(10):757-60.
15. Dhanani T, Shah S, Gajbhiye N, Kumar S. Effect of extraction methods on yield, phytochemical constituents and antioxidant activity of *Withania somnifera*. *Arab J Chem*. 2017;10:S1193-9.
16. Butkhup L, Samappito S. Changes in physico-chemical properties, polyphenol compounds and antiradical activity during development and ripening of maouang (*Antidesma bunius* L. Spreng) fruits. *J Fruit Ornament Plant Res*. 2011;19(1):85-99.
17. Recuenco MC, Lacsamana MS, Hurtada WA, Sabularse VC. Total Phenolic and Total Flavonoid Contents of Selected Fruits in the Philippines. *Philipp J Sci*. 2016;145(3):275-81.
18. Panceri CP, Gomes TM, De Gois JS, Borges DL, Bordignon-Luiz MT. Effect of dehydration process on mineral content, phenolic compounds and antioxidant activity of Cabernet Sauvignon and Merlot grapes. *Food Res Int*. 2013;54(2):1343-50.
19. Middleton Jr E, Kandaswami C. Effects of flavonoids on immune and inflammatory cell functions. *Biochem Pharmacol*. 1992;43(6):1167-79.
20. Barcelo JM, Nullar ARM, Caranto JKP, Gatchallan AM, Aquino IJB. Antioxidant and antimutagenic activities of ripe Bignay (*Antidesma bunius*) crude fruit extract. *Philipp J App Res Dev*. 2016;6:32-43
21. Jeong S-M, Kim S-Y, Kim D-R, Jo S-C, Nam K, Ahn D, Lee S. Effect of heat treatment on the antioxidant activity of extracts from citrus peels. *J Agric Food Chem*. 2004;52(11):3389-93.
22. Shaimaa G, Mahmoud M, Mohamed M, Emam A. Effect of heat treatment on phenolic and flavonoid compounds and antioxidant activities of some Egyptian sweet and chilli pepper. *Nat Prod Chem Res*. 2016;4(3):1000218.
23. Shahidi F, Yeo J. Insoluble-bound phenolics in food. *Molecules*. 2016;21(9):1216.
24. Satti J. The emerging low-dose therapy for advanced cancers. *Dose-Response*. 2009; 24;7(3):208-20.
25. Gaya A, Akle CA, Mudan S, Grange J. The concept of hormesis in cancer therapy - Is less more? *Cureus*. 2015;7(4):1-14.
26. Xie X, Wu Y, Luo S, Yang H, Li L, Zhou S, Shen R, Lin H.. Efficacy and toxicity of low-dose versus conventional-dose chemotherapy for malignant tumors: a meta-analysis of 6 randomized controlled trials. *Asian Pac J Cancer Prev*. 2017;18(2):479.
27. Lee B, Moon KM, Kim CY. Tight junction in the intestinal epithelium: Its association with diseases and regulation by phytochemicals. *J Immunol Res*. 2018;2018.
28. Martin TA, Jiang WG. Loss of tight junction barrier function and its role in cancer metastasis. *Biochim Biophys Acta*. 2009;1788(4):872-91.
29. Liou G-Y, Storz P. Reactive oxygen species in cancer. *Free Radic Res*. 2010;44(5):479-96.
30. Sumayao R, McEvoy B, Newsholme P, McMorro T. Lysosomal cystine accumulation promotes mitochondrial depolarization and induction of redox-sensitive genes in human kidney proximal tubular cells. *J Physiol*. 2016;594(12):3353-70.
31. Cuadrado A, Rojo AI, Wells G, Hayes JD, Cousin SP, Rumsey WL, Attucks OC, Franklin S, Levonen A, Kensler TW, Dinkova-Kostova AT. Therapeutic targeting of the NRF2 and KEAP1 partnership in chronic diseases. *Nat Rev Drug Discov*. 2019;18(4):295-317.
32. Zuo Q, Wu R, Xiao X, Yang C, Yang Y, Wang C, Lin L, Kong A. The dietary flavone luteolin epigenetically activates the Nrf2 pathway and blocks cell transformation in human colorectal cancer HCT116 cells. *J Cell Biochem*. 2018;119(11):9573-82.
33. Kang KA, Piao MJ, Hyun YJ, Zhen AX, Cho SJ, Ahn MJ, Yi JM, Hyun JW. Luteolin promotes apoptotic cell death via upregulation of Nrf2 expression by DNA demethylase and the interaction of Nrf2 with p53 in human colon cancer cells. *Exp Mol Med*. 2019;51(4):1-14.
34. Elmore S. Apoptosis: a review of programmed cell death. *Toxicol Pathol*. 2007;35(4):495-516.